

Enhancement of dielectric characteristics in donor doped Aurivillius $\text{SrBi}_2\text{Ta}_2\text{O}_9$ ferroelectric ceramics

Indrani Coondoo^a, A.K. Jha^{a,*}, S.K. Agarwal^b

^a Department of Applied Physics, Delhi College of Engineering, Delhi 110042, India

^b National Physical Laboratory, Dr. K. S. Krishnan Road, New Delhi 110012, India

Received 5 January 2006; received in revised form 12 April 2006; accepted 21 April 2006

Available online 11 July 2006

Abstract

In this study, investigations have been made on the crystal structure, surface morphology, dielectric and electrical properties of tungsten doped $\text{SrBi}_2(\text{W}_x\text{Ta}_{1-x})_2\text{O}_9$ ($0.0 \leq x \leq 0.20$) ferroelectric ceramics. Dielectric measurements performed as a function of temperature at 1, 10 and 100 kHz show an increase in Curie temperature (T_c) over the composition range of $x = 0.05$ – 0.20 . W^{6+} substitution in perovskite-like units results in a sharp dielectric transition at the ferroelectric Curie temperature with the dielectric constant at their respective Curie temperature increasing with tungsten doping. The dielectric loss reduces significantly with tungsten addition. The temperature dependence of ac and dc conductivity vis-à-vis tungsten content shows a decrease in conductivity, which is attributed to the suppression of oxygen vacancies. The activation energy calculated from the Arrhenius plots is found to increase with tungsten content.

© 2006 Elsevier Ltd. All rights reserved.

Keywords: Powders-solid state reaction; Electron microscopy; Dielectric properties; Electrical conductivity; $\text{SrBi}_2\text{Ta}_2\text{O}_9$

1. Introduction

The Aurivillius family of oxides with layered structure consists of regular intergrowths of $[\text{Bi}_2\text{O}_2]^{2+}$ layers with perovskite $[\text{A}_{n-1}\text{B}_n\text{O}_{3n+1}]^{2-}$ slabs.^{1,2} Generally ‘A’ is mono, di or trivalent cation that has dodecahedral coordination, whereas ‘B’ is a transition element with octahedral coordination and ‘n’ is an integer representing the number of perovskite like slabs. Role of bismuth layer in determining the electrical and ferroelectric properties of these ceramics has been found to be crucial. Bismuth layer is reported to be paraelectric in nature while perovskite unit cell structures are ferroelectric.³ Therefore, doping in these layered ceramics to improve the properties has been a matter of interest. Among the bismuth layered structure ferroelectrics (BLSFs), $\text{SrBi}_2\text{Ta}_2\text{O}_9$ (SBT), $\text{SrBi}_2\text{Nb}_2\text{O}_9$ (SBN) and their solid solutions are the better potential materials for application in information data storage such as ferroelectric random access memories (FeRAMs). They offer several advantages like being Pb-free, fatigue-free and having independence of ferroelectric proper-

ties with film thickness, as compared with isotropic perovskite ferroelectrics such as lead zirconium titanate (PZT).^{4,5}

The effect of A- and B-site substitutions in these perovskite ferroelectric materials has great relevance towards their physical and chemical properties and has been pursued intensively. Substitutional methodology has also been extensively used in piezoelectrics and ferroelectrics to improve their performance.^{6–10} Efforts on the improvement of the dielectric and ferroelectric properties are mostly based on the A-site substitutions in SBT. However, very limited work on the dielectric and electrical properties of the layered perovskite SBT vis-à-vis substitution onto the B-site ion (Ta^{5+}) with other alternate cations of higher oxidation states is available.

The present work aims at studying the effects of substitution of tungsten (W^{6+}) for tantalum (Ta^{5+}) on the structural, micro structural, dielectric and electrical properties (ac and dc conductivity) of $\text{SrBi}_2\text{Ta}_2\text{O}_9$ ferroelectric ceramics.

2. Experimental

Samples of compositions $\text{SrBi}_2(\text{W}_x\text{Ta}_{1-x})_2\text{O}_9$ (SBWT), with x ranging from 0.0 to 0.2 were synthesized by solid-state reaction method taking SrCO_3 , Bi_2O_3 , Ta_2O_5 and WO_3 (all from Aldrich)

* Corresponding author. Tel.: +91 9810361727; fax: +91 11 27871023.
E-mail address: dr_jha_ak@yahoo.co.in (A.K. Jha).

in their stoichiometric proportions. The powder mixtures were thoroughly ground and passed through sieve of appropriate size and then calcined at 900–1000 °C in air for 2 h. The calcined mixtures were ground and admixed with about 1–1.5 wt% polyvinyl alcohol (Aldrich) as a binder and then pressed at ~300 MPa into disk shaped pellets. The pellets were sintered at 1150 °C for 2 h in air.

X-ray diffractograms of both the calcined and sintered samples were recorded using a Bruker diffractometer in the range $10^\circ \leq 2\theta \leq 70^\circ$ with Cu K α radiation. Scanning Electron micrographs (SEM) for the samples were recorded using Cambridge Stereo Scan 360 microscope. The sintered pellets were polished to a thickness of ~1 mm and coated with silver paste on both the sides for use as electrodes and cured at 550 °C for half an hour. The dielectric measurements were carried out using Solartron-1260 Impedance/gain-phase analyzer operating at oscillation amplitude of 1 V. The dielectric constant as a function of temperature was measured at frequencies of 1, 10 and 100 kHz. The dc conductivity measurements were carried out in the temperature range of room temperature to 450 °C using a Keithley 6517A electrometer. DC conductivities were also calculated from the Cole–Cole plots of the various compositions to render credence to their direct measurements.

3. Results and discussion

3.1. XRD and SEM analysis

The XRD patterns of the various SBWT samples sintered at 1150 °C show similar features as reported earlier.⁶ It is observed

Table 1

The observed lattice parameters a , b and c of $\text{SrBi}_2(\text{W}_x\text{Ta}_{1-x})_2\text{O}_9$ ceramics

x	a (Å)	b (Å)	c (Å)
0.0	5.5243	5.5337	25.1001
0.025	5.5215	5.5090	24.9767
0.050	5.5172	5.5062	25.0046
0.075	5.5005	5.4807	25.0156
0.100	5.4822	5.4289	25.0354
0.200	5.4852	5.4268	25.0701

that the single phase layered perovskite structure is formed up to 5 at% of W-doping in $\text{SrBi}_2(\text{W}_x\text{Ta}_{1-x})_2\text{O}_9$. For compositions with $x > 0.05$, in addition to the major peaks representing layered perovskite phase, an unidentified peak of very low intensity is also observed which is ascribed to unreacted tungsten oxide in the material.

The peaks have been indexed using the observed interplanar spacing d and the lattice parameters so obtained were refined using the least square refinement method by a computer program package-Powdin.¹¹ On the basis of ionic radii of atoms and coordination number⁶ it is expected that tungsten atoms occupy tantalum (B) sites. This seems to be indeed the case as a decrease in the lattice constants is observed (Table 1) due to a smaller ionic radius of W^{6+} than that of Ta^{5+} .

Fig. 1 shows the SEM images of the fractured surfaces of the chemically etched undoped and doped ceramics. The average grain size of the undoped SBT is observed to be ~3–4 μm . It is observed that the average grain size and aspect ratio increased

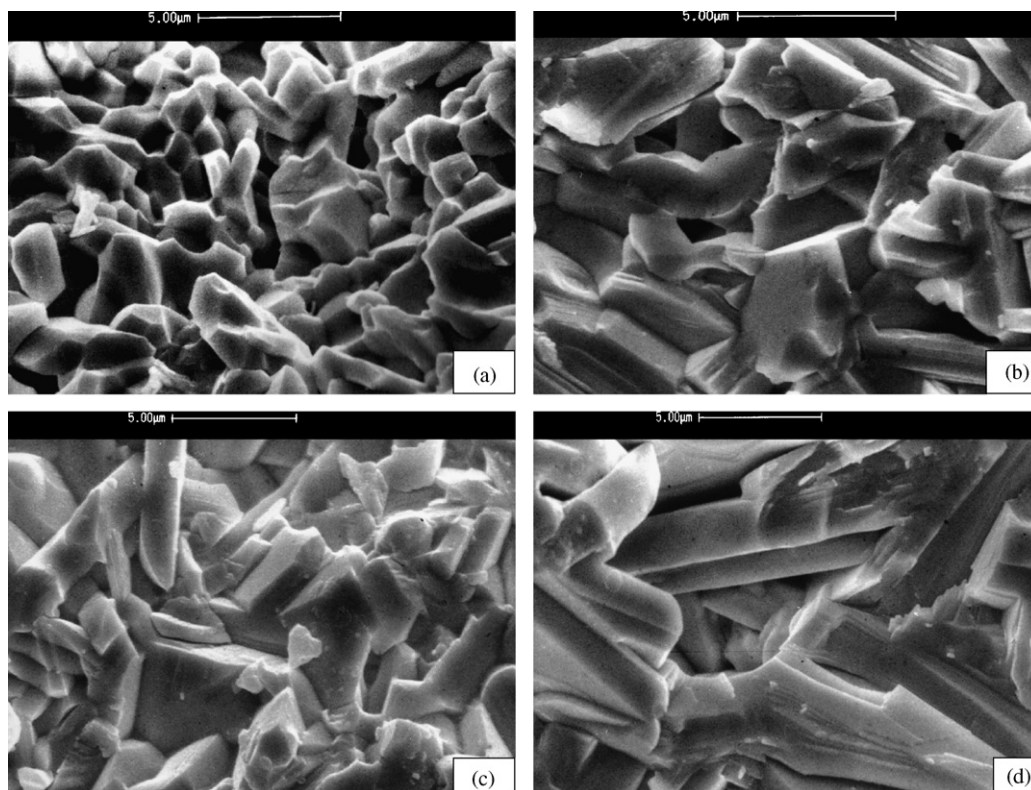


Fig. 1. SEM micrographs of fracture surface of chemically etched $\text{SrBi}_2(\text{W}_x\text{Ta}_{1-x})_2\text{O}_9$ samples: (a) $x=0.0$; (b) $x=0.025$; (c) $x=0.075$; and (d) $x=0.20$.

with the increase in tungsten content. The plate-like grains are anisotropic and randomly oriented. For the concentration range of $0.025 \leq x \leq 0.05$ the average grain size is $\sim 5\text{--}6\text{ }\mu\text{m}$ and for $0.075 \leq x \leq 0.10$ it is $\sim 4\text{--}5\text{ }\mu\text{m}$, whereas for $x=0.20$ the grain size increases to $\sim 8\text{ }\mu\text{m}$.

3.2. Dielectric properties

Fig. 2 shows the dielectric constants and dielectric loss as a function of temperature for doped and undoped ceramics measured at frequencies of 1, 10, and 100 kHz with oscillation

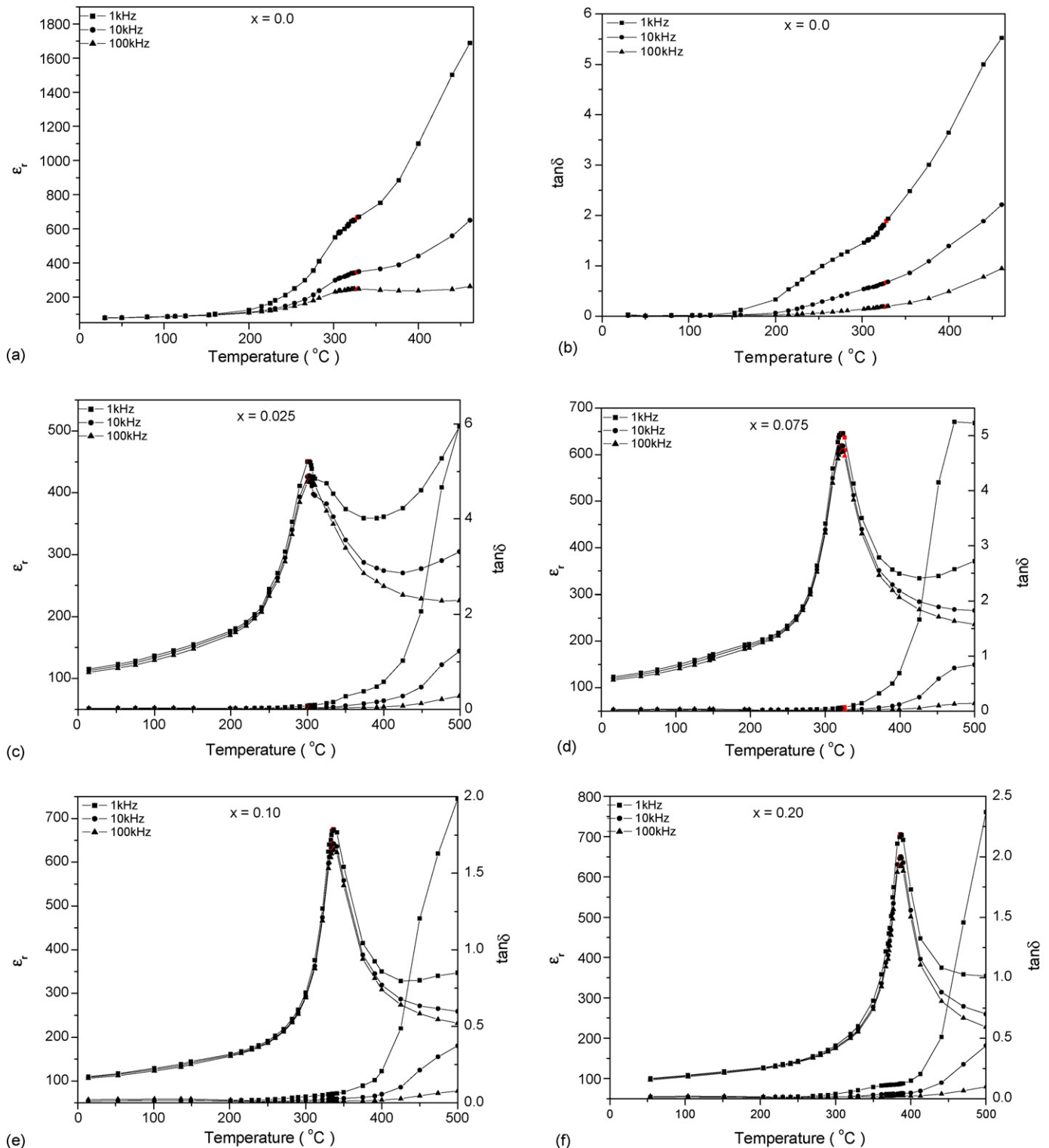


Fig. 2. Dielectric constant and dielectric loss of $\text{SrBi}_2(\text{W}_x\text{Ta}_{1-x})_2\text{O}_9$ samples as a function of temperature at 1, 10 and 100 kHz: (a) $x=0.0$; (b) $x=0.0$; (c) $x=0.025$; (d) $x=0.075$; (e) $x=0.10$; and (f) $x=0.20$.

amplitude of 1 V. For all the doped samples, a sharp transition in dielectric constant at their respective Curie temperature (T_c) is observed at all the frequencies. It is observed that the Curie temperature increases over the composition range of $x = 0.05$ – 0.20 . The dielectric constants at low temperatures for all the samples are also found to be the same regardless of the signal frequencies. The low frequency dielectric dispersion at high temperatures is observed in the case of pristine sample ($x = 0$).

It is known that the pristine $\text{SrBi}_2\text{Ta}_2\text{O}_9$ is not perfectly stoichiometric, but contains a certain amount of inherent defects (e.g. oxygen vacancies) resulting from the volatilization of Bi_2O_3 at high temperatures.¹² When Bi_2O_3 is lost, bismuth and oxygen vacancy complexes are formed in the $(\text{Bi}_2\text{O}_2)^{2+}$ layers. It has been established through X-ray photoemission spectroscopy studies that the oxygen ions in $(\text{Bi}_2\text{O}_2)^{2+}$ layers are less stable than the O^{2-} ions in $(\text{SrTa}_2\text{O}_7)^{2-}$ perovskite slabs.¹² Many investigations of $\text{Pb}(\text{Zr,Ti})\text{O}_3$ have indicated that the defects such as oxygen vacancies, $\text{V}_\text{O}^{\bullet\bullet}$, act as space charge which plays an important role in the electrical polarization of perovskite materials.^{13,14} The oxygen vacancy induced polarization becomes dominant at high temperatures and at low frequencies.¹⁴ This explains the significantly enhanced dielectric constant at low frequency and high temperatures, observed in the undoped sample (Fig. 2a). In the donor doped SBT, since the valency of the substituted cation (W^{6+}) is higher than the parent cation (Ta^{5+}), therefore substitution of two tungsten ions onto two tantalum sites creates a vacant site possibly at A-site (Sr-site) in the lattice structure so as to maintain electrical neutrality.^{15,16} Such cation vacancies effectively reduce the oxygen vacancy content and the related polarization. Therefore for higher concentration of tungsten in SBT, the low frequency dispersion at high temperatures is not observed.

The dielectric loss (at 1, 10, and 100 kHz) as a function of temperature for SBT doped with various amounts of tungsten is also shown in Fig. 2. It is observed that with tungsten doping dielectric loss reduces significantly. The source of dielectric loss in insulating ceramics is space charge polarization/domain wall relaxation.¹⁷ The presence of defects like oxygen vacancies $\text{V}_\text{O}^{\bullet\bullet}$, which act as space charge and contribute to the electrical polarization of perovskite materials, can thus be related to the dielectric loss. The undoped sample has inherent oxygen vacancies resulting from the volatilization of Bi_2O_3 , whereas with doping of W^{6+} for Ta^{5+} the formation of cation vacancies effectively reduces the concentration of oxygen vacancies. This is consistent with the observation of higher loss in case of undoped sample (Fig. 2b) and reduced loss in the doped samples (Fig. 2c–f). Similar observation of reduced loss with donor doping has also been reported by Noguchi et al.^{18,19}

Near the Curie temperature (T_c), dielectric, elastic, optical and thermal properties of the ferroelectric materials exhibit anomalous behavior. In this work, the phase transition temperature T_c of the samples has been deduced from the temperature dependence of the dielectric constant (Fig. 2). In order to understand the effect of tungsten doping in SBT on the dielectric properties, Fig. 3 illustrating the Curie temperature and dielectric constant of all the samples (at 1, 10 and 100 kHz) as a function of doping concentration is plotted. It is observed that at all fre-

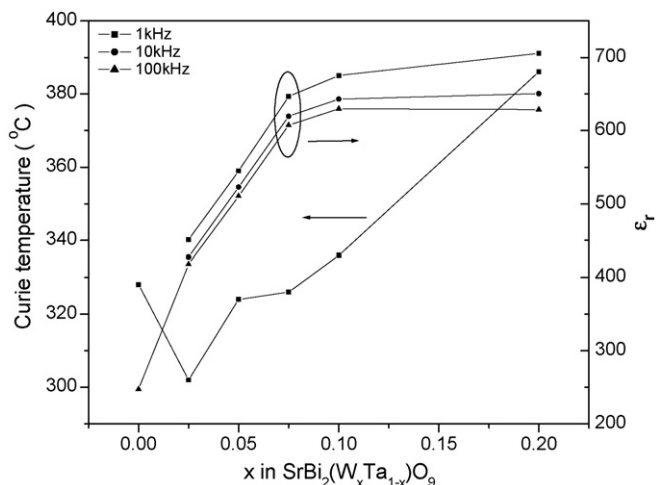


Fig. 3. The variation of Curie temperature and dielectric constant at T_c vs. concentration of tungsten in $\text{SrBi}_2(\text{W}_x\text{Ta}_{1-x})_2\text{O}_9$ at 1, 10 and 100 kHz.

quencies the T_c value for each of the doped samples remains the same. A shift in T_c to higher temperatures and a corresponding increase in peak dielectric constant with increasing concentration of tungsten is also observed. In isotropic perovskite ferroelectrics, doping at B-site (located inside an oxygen octahedron) with smaller ions results in the shift of T_c to a higher temperature, leading to a larger polarization which can be well explained by the enlarged “rattling space” available for smaller B-site ions.^{20,21} In layered-structure perovskite, the crystal structure may not change as freely as that of isotropic perovskites with doping due to the structural constraint imposed by the $(\text{Bi}_2\text{O}_2)^{2+}$ interlayer. When the dopant concentration is low, the lattice structure under the constraint and the cation vacancies at the A-site possibly have resulted in an increased stress value. In such a situation the perovskite structure would be less stable and would cause a decrease in T_c , explaining the observed decrease in T_c at $x = 0.025$ (Fig. 3). For W concentration $x > 0.05$, it is observed that the decrease in the lattice parameters a and b (Table 1) is much greater than at lower x values (< 0.05), indicating that the shrinking tendency of the crystal lattice overcomes the structural constraint imposed by the $(\text{Bi}_2\text{O}_2)^{2+}$ interlayer. Thus for higher W concentrations, decrease in the unit cell volume and introduction of cation vacancies at the A-site possibly lead to an enhancement of ferroelectric structural distortion and an eventual increase in T_c value. Enhancements in T_c value due to such factors have been reported by Wu et al.¹⁵ Higher T_c value, which is indicative of enhanced polarizability, explains the increase in dielectric permittivity with tungsten concentration (Fig. 3). Also, the cation vacancies introduced into the unit structure make the domain motion easier and increase the dielectric permittivity.^{16,22} This is supported by the grain size variation in the micrographs (Fig. 1). One expects the walls to be quite free in large grains and to be inhibited in their movement as the grain size decreases, since grain boundaries will contribute additional pinning points for the moving walls.²³ The doping of tungsten causes an overall increase in the grain size, making the domain wall motion easier and an increase in the dielectric permittivity.

3.3. AC and DC conductivity

Electrical conductivity, which directly relates to power losses is an important physical parameter and appreciably restricts the utilization of several properties of ferroelectrics.²⁴ The total conductivity σ_{tot} of the material comprises of the dc conductivity, σ_{dc} and the ac conductivity, σ_{ac} ,

$$\sigma_{\text{tot}} = \sigma_{\text{dc}} + \sigma_{\text{ac}}(\omega) \quad (1)$$

The σ_{dc} accounts for the free charges available and is independent of the frequency. The σ_{ac} accounts for the bound and free charges and can be expressed in terms of the dielectric constant ϵ_r and the dissipation factor $\tan \delta$ as:²⁵

$$\sigma_{\text{ac}} = \omega \epsilon_0 \epsilon_r \tan \delta \quad (2)$$

where ω is the angular frequency and ϵ_0 the free-space permittivity.

The plots of dc conductivity for $\text{SrBi}_2(\text{W}_x\text{Ta}_{1-x})_2\text{O}_9$ as a function of temperature are depicted in Fig. 4. The nature of curve shows that the conductivity increases with temperature. This suggests the presence of negative temperature co-efficient

of resistance (NTCR), a characteristic of insulators.²⁵ It is observed that donor doping in SBT resulted in reduced dc conductivities. Two predominant conduction mechanisms indicated by slope changes in two different temperature regions are observed. It is worth mentioning here that pure ionic conductors are expected to exhibit appreciable conductivity due to the ions present, at all temperatures. Mixed conductors, as in the present case, would however, show negligible ionic conductivity at lower temperatures ($<300^\circ\text{C}$) and therefore, the ionic conductivity in these materials would exhibit its predominance only at high temperatures. $\ln \sigma_{\text{dc}}$ Vs $10^3/T$ plots (Fig. 4a–d) for various samples clearly show two distinct slopes separating the predominance of ionic contribution in the high temperature regime. Such change in the slopes in the vicinity of the ferro-paraelectric transition region have been observed for other ferroelectrics also.^{26,27} The temperature region of ~ 300 to $\sim 700^\circ\text{C}$ in these ceramics corresponds to the intrinsic ionic conduction range where conduction is presumably dominated by the intrinsic defects.^{27,28} Table 2 summarizes the dc conductivity and activation energy values calculated using the Arrhenius equation:

$$\sigma = \sigma_0 e^{E_a/KT} \quad (3)$$

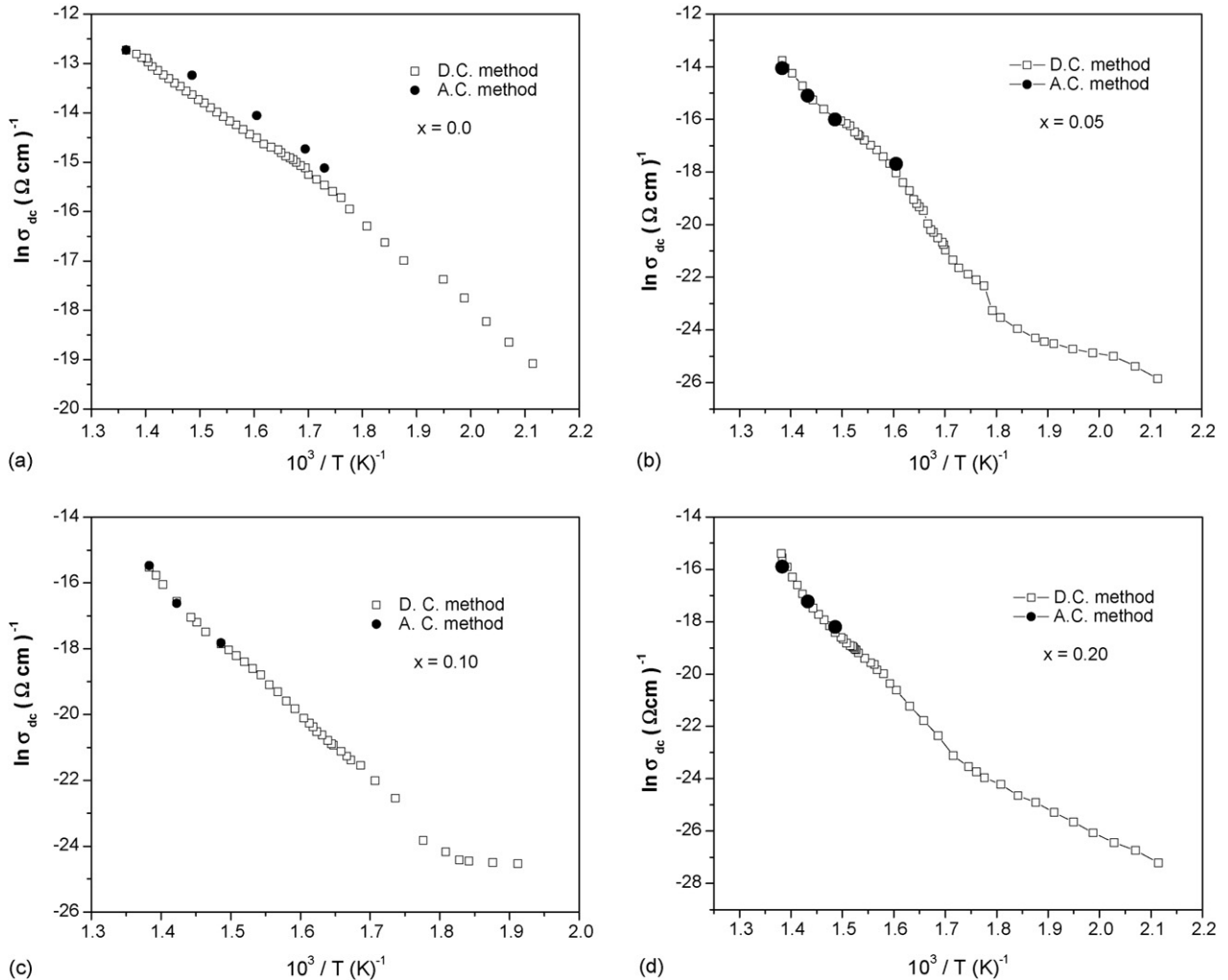


Fig. 4. The variation of dc conductivity in $\text{SrBi}_2(\text{W}_x\text{Ta}_{1-x})_2\text{O}_9$ as a function of temperature: (a) $x = 0.0$; (b) $x = 0.050$; (c) $x = 0.10$; and (d) $x = 0.20$.

Table 2
Activation energy and dc conductivity of $\text{SrBi}_2(\text{W}_x\text{Ta}_{1-x})_2\text{O}_9$ ceramics

x	Activation energy (E_a) (eV)	σ_{dc} 450 °C ($\times 10^{-7}$ S/cm)
0.0	0.690	29.63
0.025	1.977	11.96
0.050	1.951	11.91
0.075	1.987	10.55
0.100	1.725	1.807
0.200	1.723	1.738

where σ indicates the conductivity, E_a the activation energy and K the Boltzman constant. We have also calculated the dc conductivity values for various samples through their respective Cole–Cole plots (ac impedance method) at different temperatures, which closely match with the measured dc values (dc method), giving credence to the observed data (Fig. 4a–d).

The oxygen vacancy $V_{\text{O}}^{\bullet\bullet}$ is doubly positively charged with respect to the neutral lattice and is considered to be the most mobile intrinsic ionic defect in the perovskite oxides.^{29,30} Their motion in perovskites is evidenced through enhanced conductivity and activation energy of ~ 1 eV.³¹ From the shape of the

Arrhenius plot for $x=0.0$ (Fig. 4a) and the activation energy value (Table 2), it seems that the conductivity is basically due to the oxygen vacancies. In doped SBT, to achieve charge neutrality, the substitution of W^{6+} onto Ta^{5+} would be accompanied by the formation of cation vacancies and subsequent elimination of oxygen vacancies resulting in a significant decrease of vacancy complexes formed due to Bi_2O_3 volatilization. It is this decrease in the oxygen vacancy content that a decrease in conductivity with increase in concentration of tungsten is observed (Fig. 4b–d). A few other studies on layered perovskite have also reported a decrease in conductivity with addition of donors.^{27,28,32} The observed variation of conductivity with tungsten concentration in SBT is consistent with dielectric loss, which also reduces with increasing tungsten concentration and has been explained in light of contribution from the oxygen vacancies.

The ac electrical conductivity and activation energies (E_a) of the samples were calculated using Eqs. (2) and (3), respectively. The variation of ac conductivity as a function of temperature at frequencies of 1, 10 and 100 kHz is shown in Fig. 5 and the E_a of the samples are summarized in Table 3. The ferroelectric phase transitions in $\text{SrBi}_2(\text{W}_x\text{Ta}_{1-x})_2\text{O}_9$ manifests as

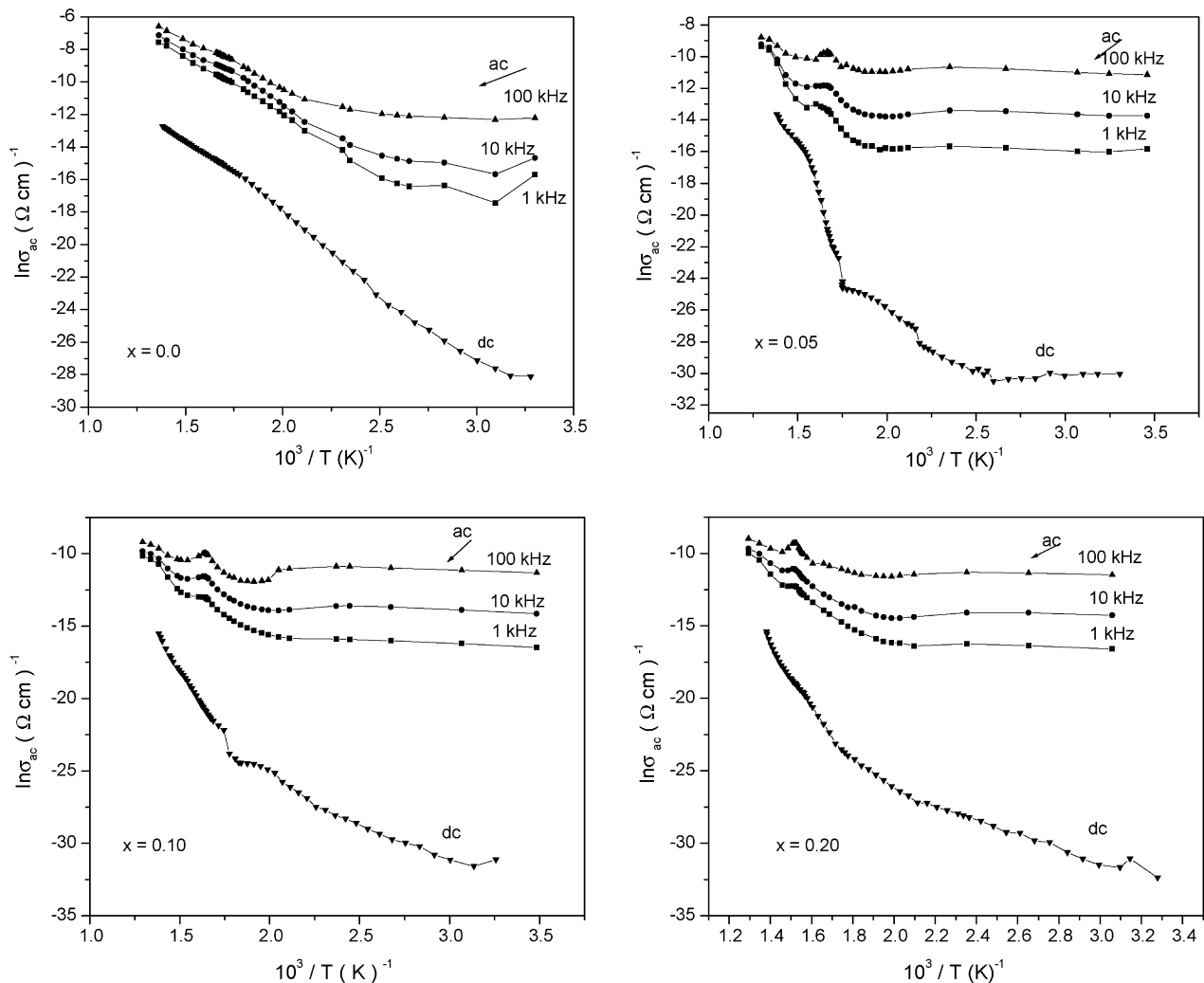


Fig. 5. The variation of ac and dc conductivity in $\text{SrBi}_2(\text{W}_x\text{Ta}_{1-x})_2\text{O}_9$ as a function of temperature.

Table 3

Activation energy (ac conductivity) of $\text{SrBi}_2(\text{W}_x\text{Ta}_{1-x})_2\text{O}_9$ ceramics

x	Activation energy (E_a) for $T > T_c$		
	1 kHz (eV)	10 kHz (eV)	100 kHz (eV)
0.0	0.589	0.481	0.429
0.025	1.123	0.924	0.642
0.050	1.872	1.225	0.529
0.075	0.998	0.946	0.428
0.100	0.936	0.842	0.613
0.200	1.314	0.863	0.511

a peak for all the samples with $x \geq 0.025$ whereas for $x = 0.0$, a mere slope change is observed around T_c . For $x = 0.0$, the dielectric and dc conductivity studies indicate the presence of oxygen vacancies. As frequency decreases, oxygen vacancies become active and mask the growth of the ferroelectric phase and hence no clear anomalies appear either in the temperature dependence of the dielectric constant or conductivity (ac and dc). At low temperatures, the ac conductivity is seen to be almost independent of temperature but shows different values at various frequencies indicating that main contribution to the conductivity result from the presence of space charges. As the temperature increases, the conductivity shows an increase with all curves tending to merge at high temperatures. Different slope changes appear in different regions of temperature, indicating the involvement of multiple activation processes with different energies.

4. Conclusions

Increase of Curie temperature is observed with tungsten concentration in the range $0.05 \leq x \leq 0.20$. The peak dielectric constant at the Curie temperature is found to increase with increasing concentration of tungsten. The dielectric loss reduces significantly on the introduction of tungsten into the parent structure SBT. The doping of tungsten into SBT is found to be effective in eliminating oxygen vacancies that decreased the conductivity by as much as two to three orders of magnitude. Such compositions should be excellent materials for highly stable ferroelectric memory devices.

Acknowledgements

The authors sincerely thank Dr. B.P. Singh, Dr. S.K. Singhal and Mr. N.C. Soni of National Physical Laboratory, New Delhi, India for providing the experimental facilities. We also express their gratitude to Prof. S.H. Pawar of Shivaji University, for illuminating discussions. One of the authors (IC) is grateful to UGC, New Delhi for the award of Senior Research Fellowship.

References

1. Aurivillius, B., Mixed bismuth oxides with layer lattices. *Ark. Kemi*, 1949, **1**, 463–470.
2. Aurivillius, B., Mixed bismuth oxides with layer lattices. *Ark. Kemi*, 1949, **1**, 499–506.

3. Irie, H., Miyayama, M. and Kudo, T., Structure dependence of ferroelectric properties of bismuth layer-structured ferroelectric single crystals. *J. Appl. Phys.*, 2001, **90**, 4089–4094.
4. Scott, J. F. and Paz de Araujo, C. A., Ferroelectric memories. *Science*, 1989, **246**, 1400–1405.
5. Mihara, T., Yoshimori, H., Watanabe, H. and Araujo, C. A. P., Characteristics of bismuth layered $\text{SrBi}_2\text{Ta}_2\text{O}_9$ thin-film capacitors and comparison with $\text{Pb}(\text{Zr}, \text{Ti})\text{O}_3$. *Jpn. J. Appl. Phys.*, 1995, **34**, 5233–5239.
6. Coondoo, I., Jha, A. K. and Agarwal, S. K., Structural, dielectric and electrical studies in tungsten doped $\text{SrBi}_2\text{Ta}_2\text{O}_9$ ferroelectric ceramics. *Ceram. Int.*, doi:10.1016/j.ceramint.2005.07.013.
7. Das, R. R., Perez, W., Bhattacharya, P. and Katiyar, R. S., Ferroelectric properties in Ca substituted $\text{SrBi}_2\text{Nb}_2\text{O}_9$ thin films. In *Proceedings of Materials Research Society Symposium-Ferroelectric Thin Films XI Symposium*, vol. 748, 2003, pp. 141–146.
8. Duran-Martin, P., Castro, A., Millan, P. and Jimenez, B., Influence of Bi-site substitution on the ferroelectricity of the Aurivillius compound $\text{Bi}_2\text{SrNb}_2\text{O}_9$. *J. Mater. Res.*, 1998, **13**, 2565–2571.
9. Millan, P., Ramirez, A. and Castro, A., Substitution of smaller Sb^{3+} and Sn^{2+} cations for Bi^{3+} in Aurivillius-like phases. *J. Mater. Sci. Lett.*, 1995, **14**, 1657–1660.
10. Shrivastava, V., Jha, A. K. and Mendiratta, R. G., Structural distortion and phase transition studies of Aurivillius type $\text{Sr}_{1-x}\text{Pb}_x\text{Bi}_2\text{Nb}_2\text{O}_9$ ferroelectric ceramics. *Solid State Commun.*, 2004, **133**, 125–129.
11. Wu, E., *POWD, an interactive powder diffraction data interpretation and indexing program Ver2.1*. School of Physical Science, Flinders University of South Australia, Bedford Park S.A. JO42AU.
12. Park, B. H., Hyun, S. J., Bu, S. D., Noh, T. W., Lee, J., Kim, H. D., Kim, T. H. and Jo, W., Differences in nature of defects between $\text{SrBi}_2\text{Ta}_2\text{O}_9$ and $\text{Bi}_4\text{Ti}_3\text{O}_{12}$. *Appl. Phys. Lett.*, 1999, **74**, 1907–1909.
13. Friessnegg, T., Aggarwal, S., Ramesh, R., Nielsen, B., Poindexter, E. H. and Keeble, D. J., Vacancy formation in $(\text{Pb}, \text{La})(\text{Zr}, \text{Ti})\text{O}_3$ capacitors with oxygen-deficiency and the effect on voltage offset. *Appl. Phys. Lett.*, 2000, **77**, 127–129.
14. Chen, A., Zhi, Y. and Cross, L. E., Oxygen-vacancy-related low-frequency dielectric relaxation and electrical conduction in $\text{Bi}:\text{SrTiO}_3$. *Phys. Rev. B*, 2000, **62**, 228–236.
15. Wu, Y., Nguyen, C., Seraji, S., Forbess, M. J., Limmer, S. J., Chou, T. and Cao, G., Processing and properties of strontium bismuth vanadate niobate ferroelectric ceramics. *J. Am. Ceram. Soc.*, 2001, **84**, 2882–2888.
16. Wu, Y., Limmer, S. J., Chou, T. P. and Nguyen, C., Influence of tungsten doping on dielectric properties of strontium bismuth niobate ferroelectric ceramics. *J. Mater. Sci. Lett.*, 2002, **21**, 947–949.
17. Zheludev, I. S., *Physics of Crystalline Dielectrics, Electrical Properties*, vol. 2. Plenum Press, New York, 1971, p. 474.
18. Noguchi, Y. and Miyayama, M., Large remanent polarization of vanadium-doped $\text{Bi}_4\text{Ti}_3\text{O}_{12}$. *Appl. Phys. Lett.*, 2001, **78**, 1903–1905.
19. Noguchi, Y., Miwa, I., Goshima, Y. and Miyayama, M., Defect control for large remanent polarization in Bismuth Titanate ferroelectrics—doping effect of higher valent cations. *Jpn. J. Appl. Phys.*, 2000, **39**, L1259–L1262.
20. Singh, K., Bopardikar, D. K. and Atkare, D. V., A compendium of $T_c - P_s$ and $P_s - \Delta z$ data for displacive ferroelectrics. *Ferroelectrics*, 1988, **82**, 55–67.
21. Subbarao, E. C., Systematics of bismuth layer compounds. *Integr. Ferr.*, 1996, **12**, 33–41.
22. Takahashi, S. and Takahashi, M., Effects of impurities on the mechanical quality factor of lead zirconate titanate ceramics. *Jpn. J. Appl. Phys.*, 1972, **11**, 31–35.
23. Martirena, H. T. and Burfoot, J. C., Grain-size effects on properties of some ferroelectric ceramics. *J. Phys. C: Solid State Phys.*, 1976, **7**, 3162–3172.
24. Araujo, C. P., *Science and Technology of Integrated Ferroelectrics*. Taylor & Francis, New York, 2001.
25. Buchanan, R. C., *Principles of Electronic Ceramics*. Marcel Dekkar, New York, 1991.

26. Mahesh Kumar, M. and Ye, Z. G., Dielectric and electrical properties of donor- and acceptor-doped ferroelectric $\text{SrBi}_2\text{Ta}_2\text{O}_9$. *J. Appl. Phys.*, 2001, **90**, 934–941.
27. Shulman, H. S., Testorf, M., Damjanovic, D. and Setter, N., Microstructure electrical conductivity and piezoelectric properties of bismuth titanate. *J. Am. Ceram. Soc.*, 1996, **79**, 3124–3128.
28. Baiatu, T., Waser, R. and Hardtl, K. H., dc Electrical degradation of perovskite-type Titanates: III, a model of the mechanism. *J. Am. Ceram. Soc.*, 1990, **73**, 1663–1673.
29. Smyth, D. M., Charge vacancy motion in ferroelectric thin films. *Ferroelectrics*, 1991, **117**, 117–124.
30. Warren, W. L., Vanheusden, K., Dimos, D., Pike, G. E. and Tuttle, B. A., Oxygen vacancy motion in perovskite oxides. *J. Am. Ceram. Soc.*, 1995, **78**, 536–538.
31. Robertson, J., Chen, C. W., Warren, W. L. and Guttleben, C. D., Electronic structure of the ferroelectric layered perovskite $\text{SrBi}_2\text{Ta}_2\text{O}_9$. *Appl. Phys. Lett.*, 1996, **69**, 1704–1706.
32. Villegas, M., Caballero, A. C., Moure, C., Duran, P. and Fernandez, J. F., Low-temperature sintering and electrical properties of chemically W-doped $\text{Bi}_4\text{Ti}_3\text{O}_{12}$ ceramics. *J. Eur. Ceram. Soc.*, 1999, **19**, 1183–1186.